1 **Electronic supplementary information**

2

3 **Metal-organic framework @ hydrogen-bond framework as matrix for MALDI-**

4 **TOF-MS analysis of small molecules**

5

6 Shi-Jun Yin [a], Guo-Can Zheng [b], Xin Yi [c], Guang-ping Lv [c], Feng-Qing Yang [a*]

7

8 [a] Department of Pharmaceutical Engineering, School of Chemistry and Chemical

9 Engineering, Chongqing University, Chongqing 401331, China

10 [b] Analytical and Testing Center, Chongqing University, Chongqing 401331, China

11 [c] School of Food Science and Pharmaceutical Engineering, Nanjing Normal University,

12 Nanjing 210023, China

13

14 *Prof. Dr. Feng-Qing Yang, School of Chemistry and Chemical Engineering,

15 Chongqing University, Chongqing 400030, China. Phone number: +8613617650637.

16 E-mail: fengqingyang@cqu.edu.cn

17

Table of contents

Supplementary Tables

Supplementary Figures

47 naringenin.

48 **Fig. S6.** Langmuir (**a**, **c**, **e**) and Freundlich (**b**, **d**, **f**) isotherm adsorption model curves

49 of three flavonoids. **HES**, hesperetin; **NAR**, naringenin; **TAN**, tangeretin.

50 **Fig. S7.** Mass spectra and corresponding chemical structures of amino acids ((**a**) L-

51 histidine, (**b**) D-phenylalanine, and (**c**) L-arginine), antihypertensive drugs ((**d**)

52 captopril, (**e**) alprenolol, and (**f**) diltiazem), non-steroid anti-inflammatory drug ((**g**)

53 acetaminophen, (**h**) ketoprofen, and (**i**) sulindac), coumarins ((**j**) psoralen, (**k**)

54 bergapten, and (**l**) imperatorin). The amino acids were dissolved in ultrapure water and

55 the other compounds were dissolved in acetonitrile. The concentration of all analytes is

56 100 μg/mL for direct analysis.

57 **Fig. S8.** MALDI-TOF-MS spectra of 100 μg/mL of tangeretin analyzed using

58 MOF@HOF as a matrix in positive ion mode with addition of 0, 20, 40, 60, 80, and

59 100 mM of NaCl.

60 **Fig. S9.** Optical images of different matrix (2 mg/mL) dispersed on the stainless-steel

61 targets. **CHCA**, α-cyano-4-hydroxycinnamic acid; **DHB**, 2, 5-dihydroxybenzoic acid;

62 **MOF@HOF**, metal-organic framework @ hydrogen-bond framework; **SA**, sinapic

63 acid; **THAP**, 2, 4, 6-trihydroxyacetophenone.

64 **Fig. S10.** (**a**) Repeatability and (**b**) storage stability test of MOF@HOF composite,

65 based on the intensity of tangeretin ([M+H]$^+$ at m/z 373).

66 **Fig. S11.** The XRD spectra of (**a**) ZIF-8, (**b**) ZIF-67, (**c**) NH$_2$-MIL-101, and (**d**) NH$_2$-

67 MIL-125.

68 **Fig. S12.** MALDI-MS imaging analysis of the NAR, HES, and TAN distribution in the

69 peel tissue of (**a**) kumquat and (**b**) honey orange. **TAN**, tangeretin; **HES**, hesperetin;

70 **NAR**, naringenin.

71

Supplementary Methods

Materials and reagents

Ferric chloride hexahydrate ($FeCl_3 \cdot 6H_2O$, >98%), acetic acid (>99%), tetra-*n*-butyl titanate (≥98%), sodium chloride (NaCl, ≥99.5%), trifluoroacetic acid (≥99%), *N,N*-dimethyl formamide (DMF, ≥99.5%), *N,N*-dimethylacetamide (DMA, >99%), and formic acid (FA, >99.5%) were purchased from Chengdu Chron Chemicals Co., Ltd. (Sichuan, China) (http://www.chronchem.com/en/). The 1H-1,2,4-triazole-3,5-diamine (DAT, >98.0%) and acetonitrile (ACN, HPLC-grade) were purchased from Adamas-beta (Shanghai, China) (http://www.adamas-beta.com). Naphthalene-1,4,5,8-tetracarboxylic dianhydride (NTD, >98.0%) and 2-methylimidazole (98%) were purchased from Tokyo Chemical Industry Co., Ltd. (Tokyo, Japan) (https://tokyochemical.lookchem.com/). 2-aminoterephthalic acid (AMAC, ≥98%) were purchased from Shanghai DiBai Biological Technology Co., Ltd. (Shanghai, China) (http://www.chemxyz.com/). Zinc acetate dihydrate ($Zn(AC)_2 \cdot 2H_2O$, 99%), cobalt chloride hexahydrate ($CoCl_2 \cdot 6H_2O$, 99%) were purchased from Macklin (Shanghai, China) (http://www.macklin.cn/). L-histidine, D-phenylalanine, and L-arginine were purchased from TargetMol, (USA) (www.targetmol.com). Imperatorin (>98%), tangeretin (≥98%), naringenin (>98%), and hesperetin (≥98%) were purchased from Chengdu Herb Substance Co., Ltd. (Sichuan, China) (https://www.herbsubstance.com/). Captopril (>99%), atenolol (>99%), and diltiazem (>99%) were purchased from Dalian Meilun Biological Technology Co., Ltd. (Liaoning, China) (http://www.meilune.com/). Polyvinyl pyrrolidone (PVP, MW=40000), acetaminophen (≥99%), ketoprofen (≥99%), and sulindac (≥99%) were purchased from Shanghai YuanYe Biological Technology Co., Ltd. (Shanghai, China) (http://yuanyebio.bioon.com.cn/). Psoralen (>98%) and bergapten (≥98%) were purchased from Chengdu DeSiTe Biological Technology Co., Ltd. (Sichuan, China) (http://cddesite.foodmate.net/). The α-cyano-4-hydroxycinnamic acid (CHCA, ≥98%), zirconium (IV) chloride (≥99.9%) and 2,5-dihydroxyterephthalic acid (≥98%) were purchased from Shanghai Aladdin Biochemical Technology Co., Ltd. (Shanghai,

101 China) (https://www.aladdin-e.com/). The chemical structures of selected flavonoids

102 are shown in Fig. S1. Water used for all the experiments was purified by a water

103 purification system (ATSelem 1820A, Antesheng Environmental Protection

104 Equipment Co., Ltd., Chongqing, China) (http://www.atshb.com/).

Characterization of the synthesized materials

106 Scanning electron microscopy (SEM) images were obtained using a field-emission

107 scanning electron microscope (FESEM) (Quanta 650, FEI, Hillsboro, OR,

108 https://www.fei.com) at 20 kV. Transmission electron microscopy (TEM) images and

109 element distribution analysis were recorded using a JEM 2100 (JEOL Ltd. Tokyo,

110 Japan, https://www.jeol.co.jp/en/) electron microscope working at 200 kV equipped

111 with energy dispersive X-ray spectrometer (EDX). Thermogravimetric analysis (TGA)

112 was carried out on Mettler TGA/DSC1/1600LF (Mettler-Toledo AG, Analytical,

113 Switzerland, https://www.mt.com/cn/zh/home.html) from 30°C to 1000°C at a heating

114 rate of 10°C min^{-1} in N_2 gas flow. Fourier transform infrared spectra (FT-IR) were taken

115 on a Bruker Tensor 27 spectrometer (Bruker, USA, https://www.bruker.com/) between

116 4000 cm^{-1} and 400 cm^{-1} in KBr media. X-ray diffraction (XRD) patterns were obtained

117 using X'pert Powder diffractometer (Malvern Panalytical Ltd., Netherlands,

118 https://www.malvernpanalytical.com/en/) with secondary beam graphite

119 monochromated Cu Kα radiation. X-ray photoelectron spectrometer (XPS) were

120 recorded on a PHI5000 Versaprobe system using monochromatic Al Ka radiation

121 (1486.6 eV), and the obtained binding energies were referenced to the C 1s line set at

122 284.8 eV. Nitrogen sorption studies were carried out using a Quadrasorb 2MP

123 (Quantachrome, US, http://quanta.cnpowder.com.cn) specific surface and aperture

124 analyzer. Before the adsorption measurements, the samples were activated under

125 vacuum at 50°C for 24 h.

Preparation of MOF@HOF composite

127 UiO-66-(OH)$_2$ was synthesized according to the previous report with some

128 modifications [1]. Typically, ZrCl$_4$ (420 mg), H$_2$BDC-(OH)$_2$ (357 mg), and PVP (400

mg, Mw = 40000) were dissolved into a mixed solution (DMF/ultra-pure water/acetic acid = 27/1/25.6, v/v/v, 60 mL). The mixture was sonicated for 20 min, placed in a 100 mL Teflon-lined hydrothermal reaction kettle and heated at 120°C for 2 h. The material was collected by centrifugation (6790 × g, 15 min) and washed repeatedly with fresh DMF (20 mL) and methanol (20 mL) for three times, respectively. Finally, the product was dried under vacuum at 60°C for 12 h.

The MOF@HOF composite was synthesized through a solvothermal reaction. In brief, DAT (99.1 mg) and NTD (134 mg) were dispersed in DMA (20 mL), the mixture was sonicated for 5 min and followed by magnetically stirring for 1 h to obtain a homogenous solution under N_2 in an ice bath. Subsequently, UiO-66-(OH)$_2$ (100 mg) was dispersed in DMA (25 mL) and added into the above mixture, and stirred to mix well. Then, the mixture was placed in a 50 mL Teflon-lined hydrothermal reaction kettle and heated at 180°C for 12 h. The obtained product (MOF@HOF) was separated by centrifugation (6790 × g, 15 min), washed alternately with DMA (20 mL) and ACN (20 mL) for three times. Finally, the product was dried under vacuum at 50°C for 12 h.

Preparation of NH$_2$-MIL-101

NH$_2$-MIL-101 was prepared according to previous report with minor modifications [2]. FeCl$_3$·6H$_2$O (4 mM), acetic acid (3.6 mL) and 2-aminoterephthalic acid (4 mM) were added and dispersed in DMF (90 mL) under sonication for 1.0 h. Then, the mixture was transferred to in a Teflon-lined autoclave and heated to 110 °C for 24 h. The obtained product was washed with DMF (2 × 50 mL) and ethanol (2 × 50 mL), and dried under vacuum at 60 °C for 12 h. The XRD result was shown in Fig. S11a.

Preparation of NH$_2$-MIL-125

The NH$_2$-MIL-125 was prepared according to previous report with minor modifications [3]. 2-aminoterephthalic acid (10.0 mM) and tetra-n-butyl titanate (5.0 mM) were added and dispersed in mixture solution (50 mL DMF and 5 mL MeOH) under sonication for 30 min. Then, the mixture was transferred to in a Teflon-lined autoclave and heated to 150 °C for 72 h. The obtained product was washed with DMF (2 × 50 mL) and ethanol

158 (2 × 50 mL), and dried under vacuum at 60 °C for 12 h. The XRD result was shown in

159 Fig. S11b.

Preparation of ZIF-8

161 The ZIF-8 was prepared according to previous report with minor modifications [4].

162 $Zn(AC)_2 \cdot 2H_2O$ (351 mg) and 2-methylimidazole (2627 mg) were added and dispersed

163 in H_2O (48 mL) under sonication for 5 min. Then, the mixture was transferred to a

164 beaker and heated to 30 °C for 11 h. The obtained product was washed with deionized

165 water (3 × 10 mL) and dried under vacuum at 50 °C for 12 h. The XRD result was

166 shown in Fig. S11c.

Preparation of ZIF-67

168 The ZIF-67 was prepared according to previous report with minor modifications [5].

169 $CoCl_2 \cdot 6H_2O$ (519 mg), PVP (600 mg), and 2-methylimidazole (2630 mg) were added

170 and dispersed in MeOH (80 mL) under sonication for 5 min. Then, the mixture was

171 transferred to a beaker and heated to 30 °C for 12 h. The obtained product was washed

172 with MeOH (3 × 10 mL) and dried under vacuum at 50 °C for 12 h. The XRD result

173 was shown in Fig. S11d.

Adsorption experiments

175 To investigate the adsorption capacity of the MOF@HOF composite, equilibrium and

176 kinetic adsorption experiments were carried out. For equilibrium experiment, 1.0 mg of

177 adsorbent was dispersed in the mixed reference compounds solution (12.5−200 μg/mL)

178 with ultrasonication, and the mixture was shaken on a temperature-controlled air bath

179 shaker (SHZ-82, Jintan Zhengrong Experimental Instrument Factory, Jiangsu, China)

180 at 180 rpm for 25 min under 30°C to acquire adsorption equilibrium. Subsequently, the

181 equilibrium solution was filtered through a 0.22 μm filter (Shanghai Titan Scientific,

182 Shanghai, China) before HPLC analysis. For kinetic adsorption experiment, 1.0 mg of

183 adsorbent was suspended in 1.0 mL of 50 μg/mL of mixed reference compounds

184 solution. The mixtures were continuously shaken for different time (2−30 min) and the

185 concentrations of supernatant were determined. The adsorption capacity of flavonoid

186 was calculated by the following equation.

$$Q_e = \frac{(C_o - C_e)V}{m}$$

187

188 Where Q_e (mg/g) is the adsorption capacity of the adsorbent at equilibrium; C_o and C_e

189 (μg/mL) represent the initial and equilibrium solution concentration, respectively; V (L)

190 is the volume of the mixed reference compounds solution; and m (g) is the weight of

191 adsorbent added to the solution.

Chromatographic conditions

192

193 HPLC analysis was performed on an Agilent 1260 Series liquid chromatography

194 system (Agilent Technologies, Palo Alto, California, USA), which was equipped with

195 a vacuum degasser, a binary pump, an auto-sampler, and a diode array detector, and

196 was controlled by the Agilent ChemStation software. An Agilent ZORBAX SB-C18

197 column (150 × 4.6 mm i.d., 5 μm) and a pre-column (ZORBAX SB-C18 guard column,

198 12.5 × 4.6 mm i.d., 5 μm) was employed to separate HES, NAR, and TAN. The mobile

199 phase consists of formic acid-water (1:1000, v/v) (A) and acetonitrile (B) with gradient

200 elution as follows: 0−10 min, 75%−30% B; 10−11 min, 30% B; 11−12 min, 30%−75%

201 B; 12−20 min, 75% B. The flow rate of mobile phase was 1.0 mL/min, detection

202 wavelength was at 280 nm, and injection volume was 5 μL and column temperature

203 was controlled at 35°C.

Validation of the developed HPLC method

204

205 The stock solution containing the three reference compounds, including 1.0 mg/mL of

206 NAR, HES, and TAN, were prepared with ACN and stored in a brown volumetric flask

207 at 4°C. To establish the calibration curves, the stock solution was diluted to appropriate

208 concentrations (12.5−200.0 μg/mL). Different concentrations of three reference

209 compounds were injected and analyzed in triplicate. The calibration curves are peak

210 areas versus the concentrations of each compound. The limit of detection (LOD) was

211 determined as a signal-to-noise ratio equal to 3, and the limit of quantification (LOQ)

212 was determined as a signal-to-noise ratio equal to 10. The precision was evaluated by

213 intra-day and inter-day variability. Intra-day reproducibility was carried out by

214 analyzing the individual sample solution six times within one day. Inter-day variability

215 was carried out by analyzing sample solution six times in three consecutive days.

216 **Using MOF@HOF as an adsorbent and matrix**

217 A 0.1 mL MOF@HOF dispersed solution was added into a 2-mL centrifuge tube

218 containing 0.9 mL of tested sample solution, and shaken on a temperature-controlled

219 air bath shaker (SHZ-82, Jintan Zhengrong Experimental Instrument Factory, Jiangsu,

220 China) at 150 rpm for 25 min under 40°C to acquire adequate adsorption. Then, the

221 material was separated by centrifugation at $4316 \times g$ for 5 min and re-dispersed in 50

222 µL of ACN under ultrasonication. A 1 µL of solution was dropped onto the MALDI

223 stainless steel plate and dried at room temperature before MALDI-TOF MS analysis.

224 **Sample preparations**

225 The stock solutions (1.0 mg/mL) of amino acids (L-histidine, D-phenylalanine, and L-

226 arginine) were prepared by dissolving them in water, and the other analytes, including

227 HES, NAR, TAN, captopril, alprenolol diltiazem, acetaminophen, ketoprofen, sulindac,

228 psoralen, bergapten, and imperatorin were prepared by dissolving their reference

229 compounds in ACN. These solutions were freshly prepared and use (diluted to the

230 desired concentration) within three days.

231 The traditional matrices, including CHCA, DHB, SA, and THAP, were prepared

232 as saturated solutions in ACN/water (1:1, v/v) containing 0.1% of trifluoroacetic acid

233 at the final concentration of 10 mg/mL. The MOF@HOF matrix was dispersed in ACN

234 to form a homogeneous solution at the concentration of 2 mg/mL.

235 The 1.2 g of kumquat (*Fortunella margarita*, Guangxi, China) and honey orange

236 (*Citrus sinensis*, Guangxi, China) peels were accurately weighed and placed in a 50 mL

237 conical flask with stopper, respectively. Then, the fruit peels were extracted with 10

238 mL of ACN for 5 min under ultrasonication, respectively. The extract was centrifuged

239 at $6790 \times g$ for 10 min, and the supernatant was filtered through 0.22 μm microporous

240 membrane and stored at 4°C before analysis.

241 **MALDI-TOF-MS analysis**

242 All MALDI-TOF-MS measurements were performed on an MALDI-7090 (Shimadzu

Scientific Instruments, Kyoto, Japan) equipped with a pulsed nitrogen laser (355 nm) in reflection and positive ion mode. The main parameters are as follows: raster type, regular circle; profiles, 100 profiles; accumulate, 50 laser shots fired at 50 Hz. A polished-steel sample target with 384 spots was employed and laser intensity was adjusted to 40%.

For the direct analysis using MOF@HOF as a matrix. The 100 µL of MOF@HOF solution (2 mg/mL) was added into a 2-mL centrifuge tube containing 900 µL of tested sample solution. After ultrasonic dispersion for 5 min, 1 µL of the solution was dropped onto the MALDI stainless steel plate and dried at room temperature for MALDI-TOF-MS analysis. On the other hand, for the enrichment treatment using MOF@HOF as an adsorbent before MS analysis. The 100 µL of MOF@HOF solution (2 mg/mL) was added into a 2-mL centrifuge tube containing 900 µL of tested sample solution and shaken on a temperature-controlled air bath shaker (SHZ-82, Jintan Zhengrong Experimental Instrument Factory, Jiangsu, China) at 150 rpm for 25 min under 40°C to acquire adequate adsorption. Then, the material was separated by centrifugation at 6790 $\times$ g for 5 min and re-dispersed in 50 µL ACN under ultrasonication. Finally, 1 µL of the solution was dropped onto the MALDI stainless steel plate and dried at room temperature for MALDI-TOF-MS analysis.

Section of pericarp tissue and MALDI-MSI analysis

Fresh samples of kumquat and honey orange were stored at -20°C. For the analysis of distribution of flavonoids in peel tissue, peels of fruits were cut into 18 µm slices using a LEICA CM1950 freezing microtome (LEICA Microsystems GmbH, Intertzlar, Germany) at -20°C. MSI analysis was performed on an UltrafleXtreme MALDI TOF/TOF MS (Bruker Daltonics, USA) equipped with a frequency tripled Nd: YAG solid-state laser (355 nm). Tissue sections were analyzed in positive reflection ion mode with 100 laser shots fired at 1000.0 Hz. MSI data was analyzed using FlexAnalysis 3.4 and FlexImaging 4.1 (Bruker Daltonics).

Supplementary Results

To meet the requirement of adsorption kinetics and isotherm experiments test, a HPLC method of a wide linear range (12.5−200.0 μg/mL) was developed. Fig. S4 shows the fitting curves of three flavonoids and Table S2 shows the analytical performance parameters of the method, the relatively high correlation coefficient ($R^2 \geq 0.9991$) were obtained within the tested range. The LODs and LOQs are in the ranges of 6.9−10.3 ng/mL and 20.7−30.9 ng/mL, respectively. The RSDs of intra- and inter-day repeatability are in the range of 0.8%−1.6%, 1.9%−2.5%, respectively.

To evaluate the adsorption properties of the material, adsorption kinetics and isotherm experiments were carried out. The adsorption isotherms for adsorbent to flavonoids at room temperature are shown in Fig. S5a. The adsorption capacity continuously increased with increasing initial concentration at the beginning of adsorption process, thereafter, the adsorption capacity achieved saturation when the initial concentrations of flavonoids were 200 μg/mL. The highest adsorption capacity of the adsorbent to NAR, HES, and TAN were obtained to be 11.8, 18.5, and 29.0 mg/g, respectively. To further study the binding properties, the Langmuir and Freundlich models were selected to fit the obtained experimental data. As expected, the Langmuir model equation is much better for modeling the isotherm adsorption than the Freundlich model equation (Fig. S6, Table S3), which can be concluded that the recognition sites are uniformly distributed in a monolayer on the adsorbent surface. The adsorption kinetic curves for adsorbent to flavonoids of different adsorption time are shown in Fig. S5b. The adsorption capacity of adsorbent increased gradually with time and reached equilibrium at 25 min. The fast equilibrium may be related to the high specific surface area and high porosity of the material. The results revealed that the adsorption of flavonoids on MOF@HOF can quickly reach an adsorption equilibrium with a satisfactory adsorption capacity.

Reference

[1] S. J. Yin, X. Wang, H. Jiang, M. Lu, X. Zhou, L. X. Li, F. Q. Yang, *Anal. Bioanal.*

300 *Chem.*, 2021, **413**, 6987−6999.

301 [2] J. Guo, Y. Wan, Y. F. Zhu, M. T. Zhao, Z. Y. Tang, *Nano Res.*, 2021, **14**,

302 2037−2052.

303 [3] R. Bibi, H. L. Huang, M. Kalulu, Q. H. Shen, L. F. Wei, O. Oderinde, N. X. Li, J.

304 C. Zhou, *ACS Sustain Chem Eng.*, 2019, **7**, 4868-4877.

305 [4] Z. J. Zhang, S. K. Xian, H. X. Xi, H. H. Wang, Z. Li, *Chem. Eng. Sci.* 2011, **66**,

306 4878−4888.

307 [5] J. Tang, R. R. Salunkhe, J. Liu, N. L. Torad, M. Imura, S. Furukawa, Y. Yamauchi,

308 *J. Am. Chem. Soc.*, 2015, **137**, 1572−1580.

309

310

Table S1. Method validation using MOF@HOF as a matrix for the direct analysis of three flavonoids by MALDI-TOF-MS

Analytes	Regressive curves	Liner range ($\mu g \cdot mL^{-1}$)	R^2	LOD ($\mu g/mL$)	LOQ ($\mu g/mL$)	RSD (%) (*n*=6)
NAR	Y=4.32X+84.22	25−200	0.9986	7.0	23.4	11.1
HES	Y=5.62X+156.11	25−200	0.9993	5.3	17.8	9.9
TAN	Y=45.19X+412.72	25−200	0.9968	1.1	3.7	7.8

HES, hesperetin; **NAR**, naringenin; **TAN**, tangeretin.

Table S2. Analytical performance for the determination of the investigated flavonoids by the developed HPLC method

Analytes	Regressive curves	Liner range ($\mu g \cdot mL^{-1}$)	R^2	LOD (ng/mL)	LOQ (ng/mL)	Intra-day RSD (%) (*n*=6)	Inter-day RSD (%) (*n*=6)
NAR	Y=91.63X+235.63	12.5−200.0	0.9991	10.3	30.9	1.6	2.0
HES	Y=76.61X+111.69	12.5−200.0	0.9998	8.2	24.7	1.4	1.9
TAN	Y=70.31X+59.62	12.5−200.0	0.9999	6.9	20.7	0.8	2.5

HES, hesperetin; **NAR**, naringenin; **TAN**, tangeretin.

Table S3. The linear relationship and parameters of Langmuir and Freundlich adsorptions

Compounds	Langmuir				Freundlich			
	Regressive equation	Q_m (mg g^{-1})	K_l (mL mg^{-1})	R^2	Regressive equation	$K_f(mg^{1-\frac{1}{n}}L^{\frac{1}{n}}g^{-1})$	$\frac{1}{n}$ a	R^2
TAN	Y=0.259X+0.067	30.3	0.04	0.996	Y=2.015X-1.622	0.02	2.015	0.824
HES	Y=0.647X+0.055	18.2	0.09	0.998	Y=2.073X-1.133	0.07	2.073	0.763
NAR	Y=0.746X+0.033	14.9	0.26	0.998	Y=2.035X+0.162	1.45	2.035	0.916

a: 0.1 <1/n≤0.5 represented that the adsorption is very easy to perform; 0.5 <1/n≤1 represented that the adsorption is easy to perform; 1>1/n represented that the adsorption is difficult to perform. **HES**, hesperetin; **NAR**, naringenin; **TAN**, tangeretin.

Table S4. Method validation using MOF@HOF as an adsorbent and matrix for the analysis of three flavonoids by MALDI-TOF-MS

Analytes	Regressive curves	Liner range (ng·mL^{-1})	R^2	LOD (ng/mL)	LOQ (ng/mL)	RSD (%) (n=6)
NAR	Y=11.31X+150.51	10−100	0.9926	2.7	9.0	10.9
HES	Y=19.34X+109.09	10−100	0.9964	2.0	6.7	7.5
TAN	Y=147.66X+545.31	10−100	0.9936	0.3	1.1	4.3

Table S5. Determination of three flavonoids in kumquat and honey orange by MALDI-TOF-MS using MOF@HOF as an adsorbent and matrix

Sample	Real content (ng mL⁻¹)			Spiked level (ng mL⁻¹)	Found (ng mL⁻¹)			Recovery (%)		
	NAR	HES	TAN		NAR	HES	TAN	NAR	HES	TAN
Kumquat	10.1	-	18.7	20	29.8±1.1	16.4±0.7	35.5±2.5	99.2±3.5	82.2±3.3	91.7±6.5
				50	55.6±2.0	47.0±1.9	65.4±4.6	92.5±3.4	94.1±3.9	95.2±6.7
				80	86.9±1.6	75.3±1.6	95.8±2.6	96.4±1.7	94.2±2.1	97.1±2.6
Honey orange	-	15.7	10.5	20	17.2±1.2	31.6±1.0	28.1±3.0	86.2±6.0	88.5±2.7	92.2±9.8
				50	45.9±1.9	62.0±1.2	61.3±2.7	91.9±3.8	94.4±1.8	101.4±4.5
				80	75.8±2.0	84.4±4.9	89.1±4.2	94.8±2.6	88.2±5.1	98.4±4.7

Naringenin   **Hesperetin**   **Tangeretin**
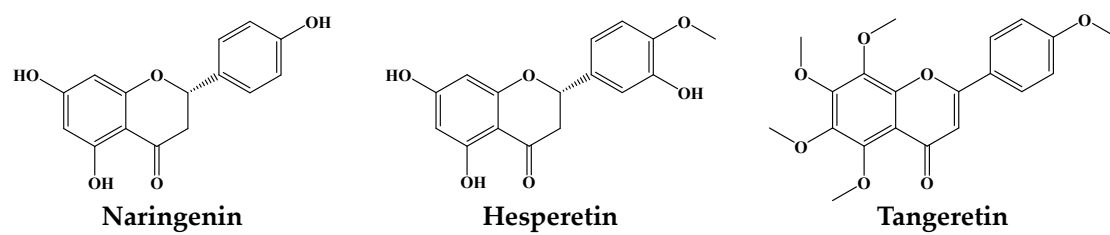
Fig. S1. Chemical structures of selected flavonoids.
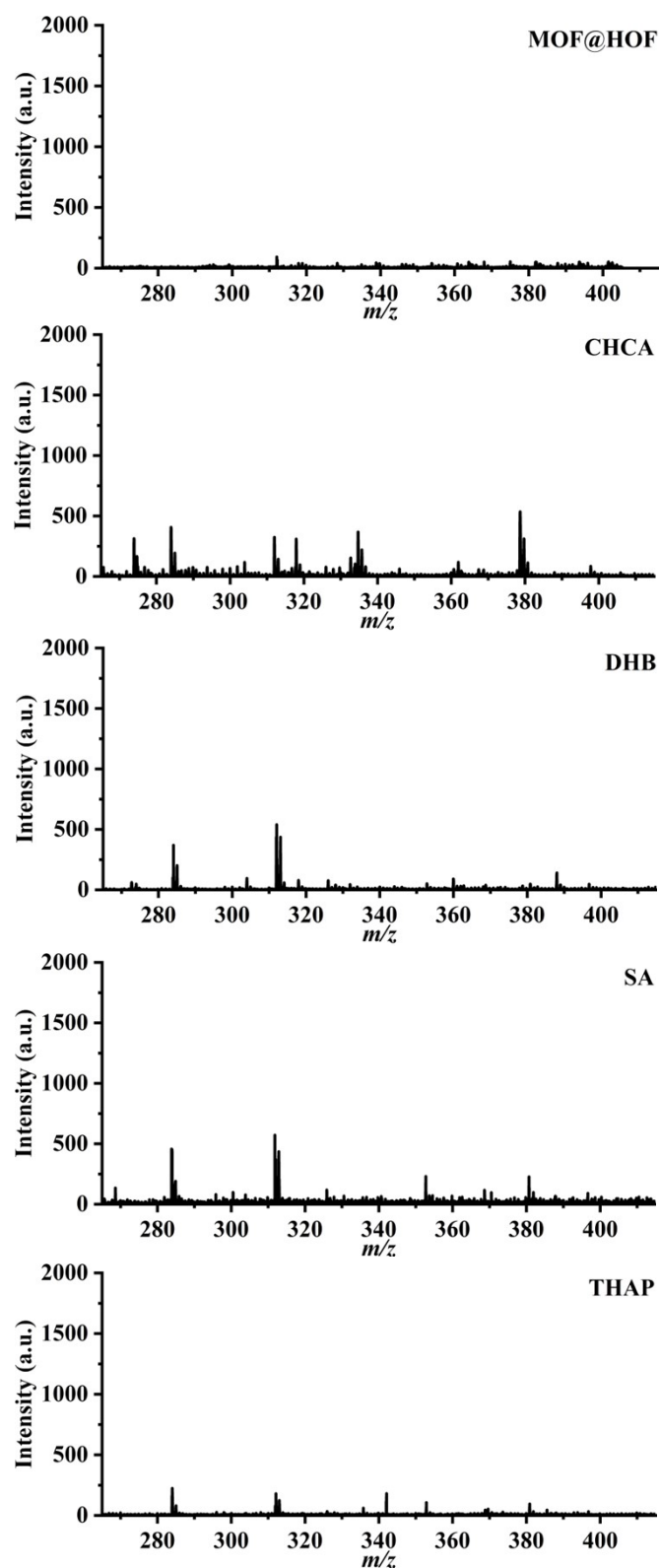
Fig. S2. The background mass spectra of MOF@HOF composite and traditional matrix. **CHCA**, α-cyano-4-hydroxycinnamic acid; **DHB**, 2, 5-dihydroxybenzoic acid; **MOF@HOF**, metal-organic framework @ hydrogen-bond framework; **SA**, sinapic acid; **THAP**, 2, 4, 6-trihydroxyacetophenone.
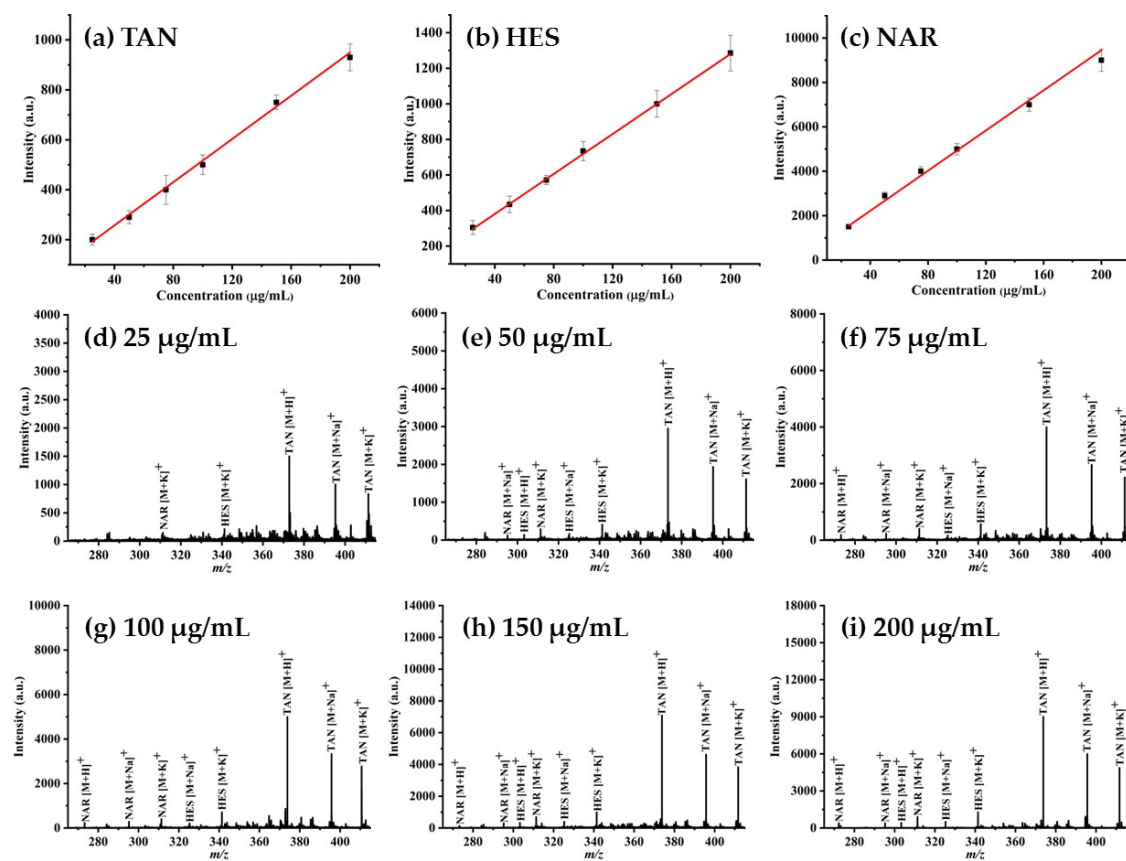
Fig. S3. The calibration curves of (**a**) TAN, (**b**) HES, and (**c**) NAR using MOF@HOF as a matrix for the direct MALDI-TOF-MS analysis, based on the intensity of TAN ([M+H]$^+$ at *m/z* 373), HES ([M+K]$^+$ at *m/z* 341), and NAR ([M+K]$^+$ at *m/z* 311); (**d−i**) Mass spectra of mixed reference compounds in the concentrations of 25−200 μg/mL. **HES**, hesperetin; **NAR**, naringenin; **TAN**, tangeretin.
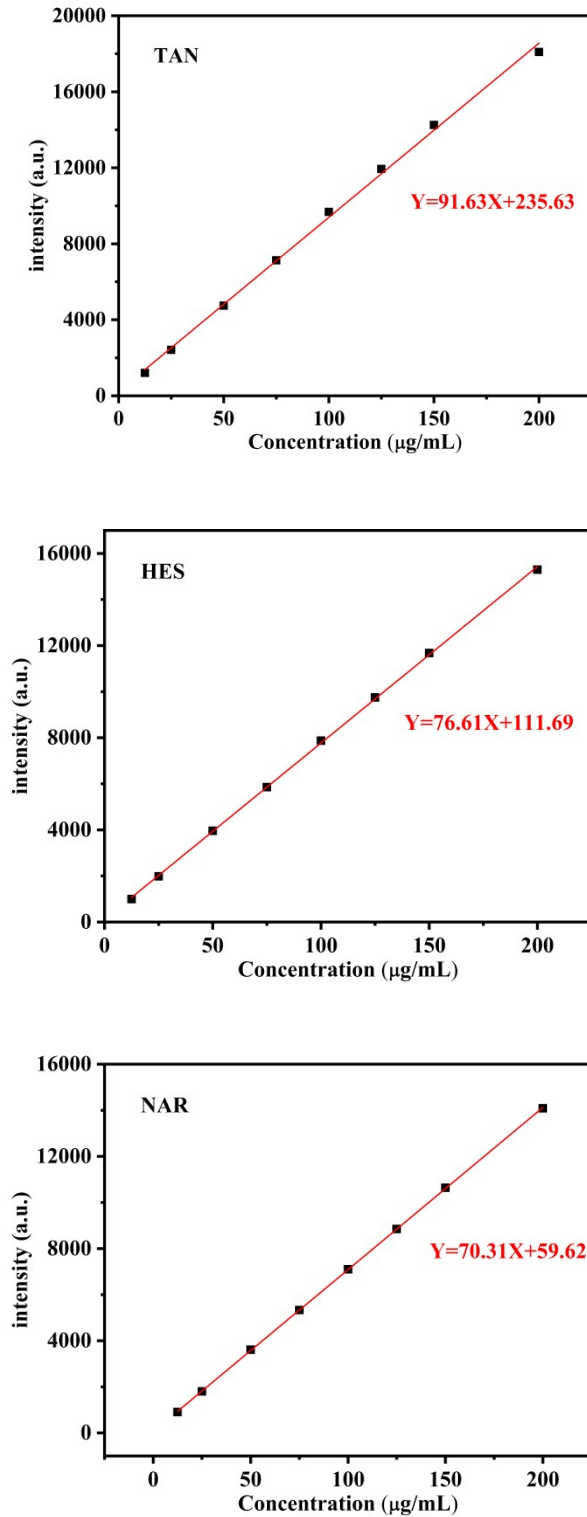
Fig. S4. The calibration curves of investigated flavonoids determined by HPLC using MOF@HOF as an adsorbent. **HES**, hesperetin; **NAR**, naringenin; **TAN**, tangeretin.
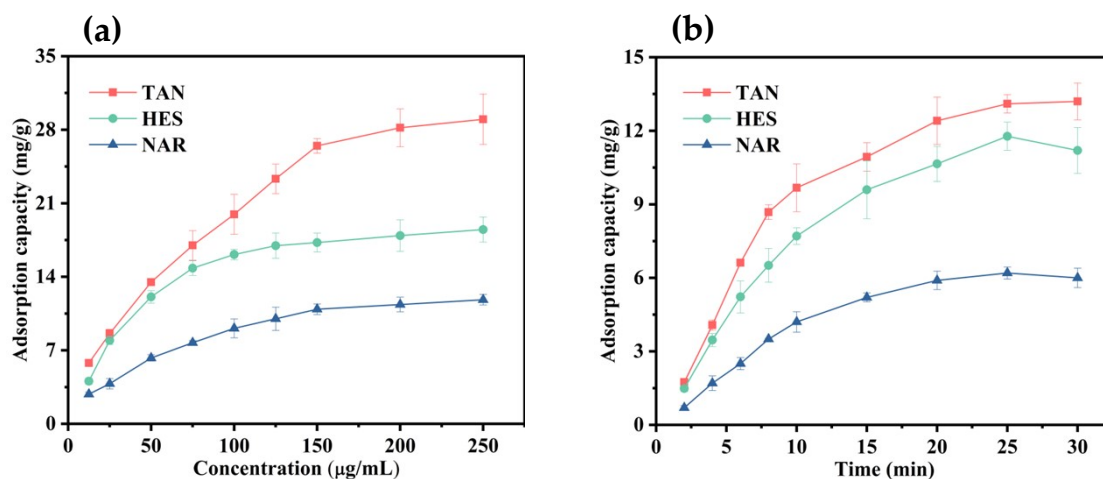
Fig. S5. (**a**) Adsorption isotherms and (**b**) adsorption kinetics of TAN, HES, and NAR using MOF@HOF as an adsorbent. TAN, tangeretin; HES, hesperetin; NAR, naringenin.
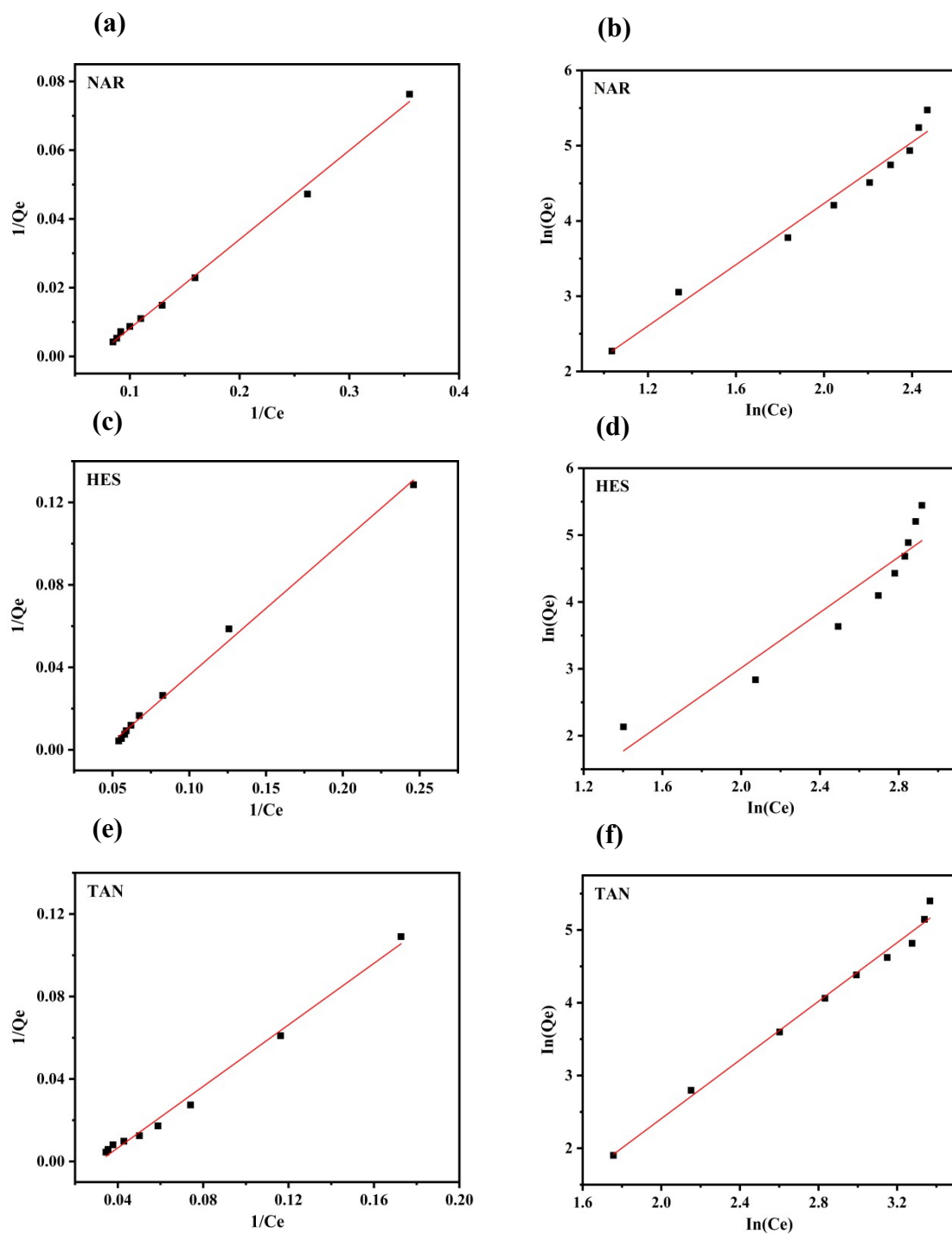
Fig. S6. Langmuir (**a**, **c**, **e**) and Freundlich (**b**, **d**, **f**) isotherm adsorption model curves of three flavonoids. **HES**, hesperetin; **NAR**, naringenin; **TAN**, tangeretin.
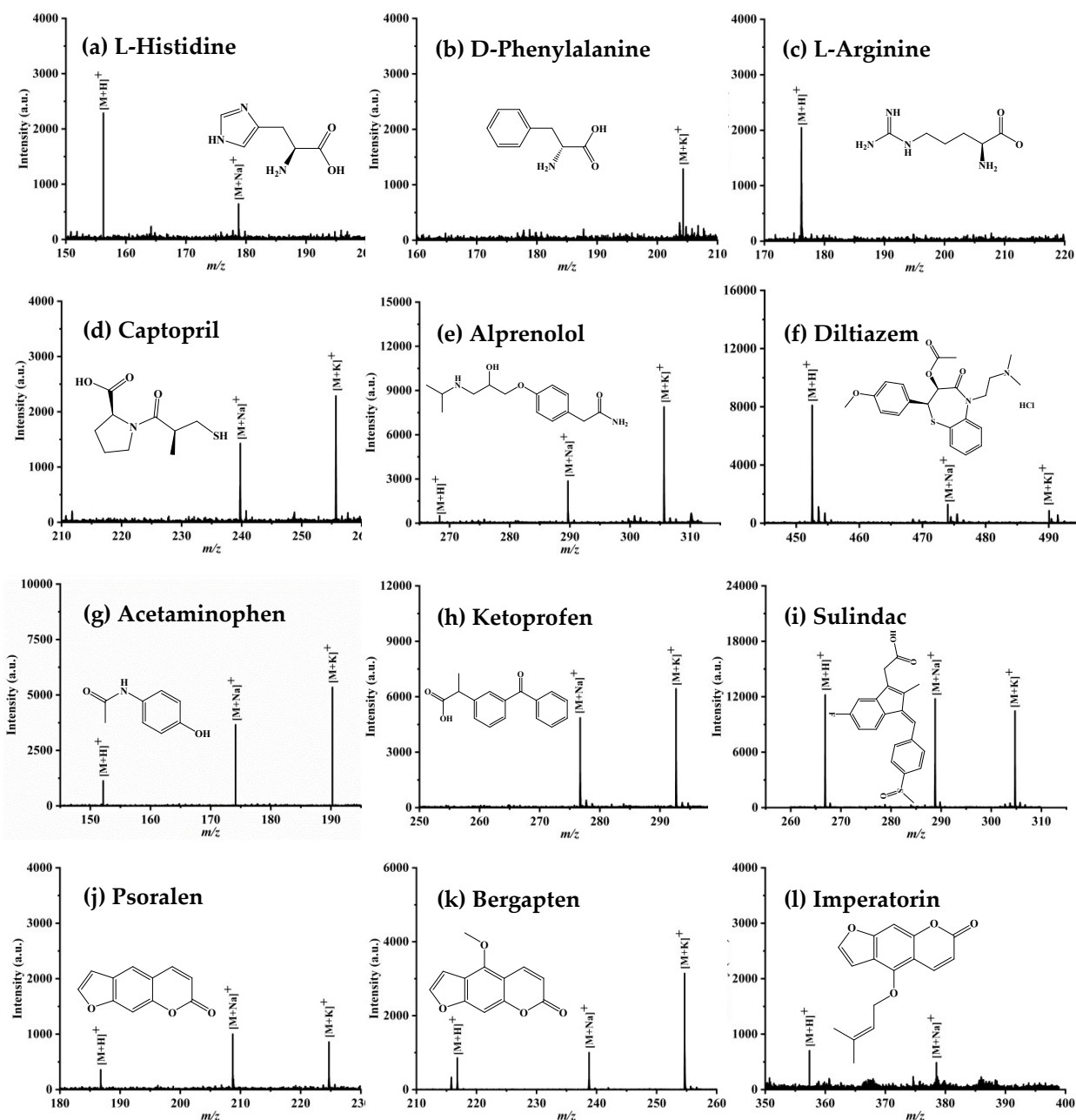
Fig. S7. Mass spectra and corresponding chemical structures of amino acids ((**a**) L-histidine, (**b**) D-phenylalanine, and (**c**) L-arginine), antihypertensive drugs ((**d**) captopril, (**e**) alprenolol, and (**f**) diltiazem), non-steroid anti-inflammatory drug ((**g**) acetaminophen, (**h**) ketoprofen, and (**i**) sulindac), coumarins ((**j**) psoralen, (**k**) bergapten, and (**l**) imperatorin). The amino acids were dissolved in ultrapure water and the other compounds were dissolved in acetonitrile. The concentration of all analytes is 100 μg/mL for direct analysis.
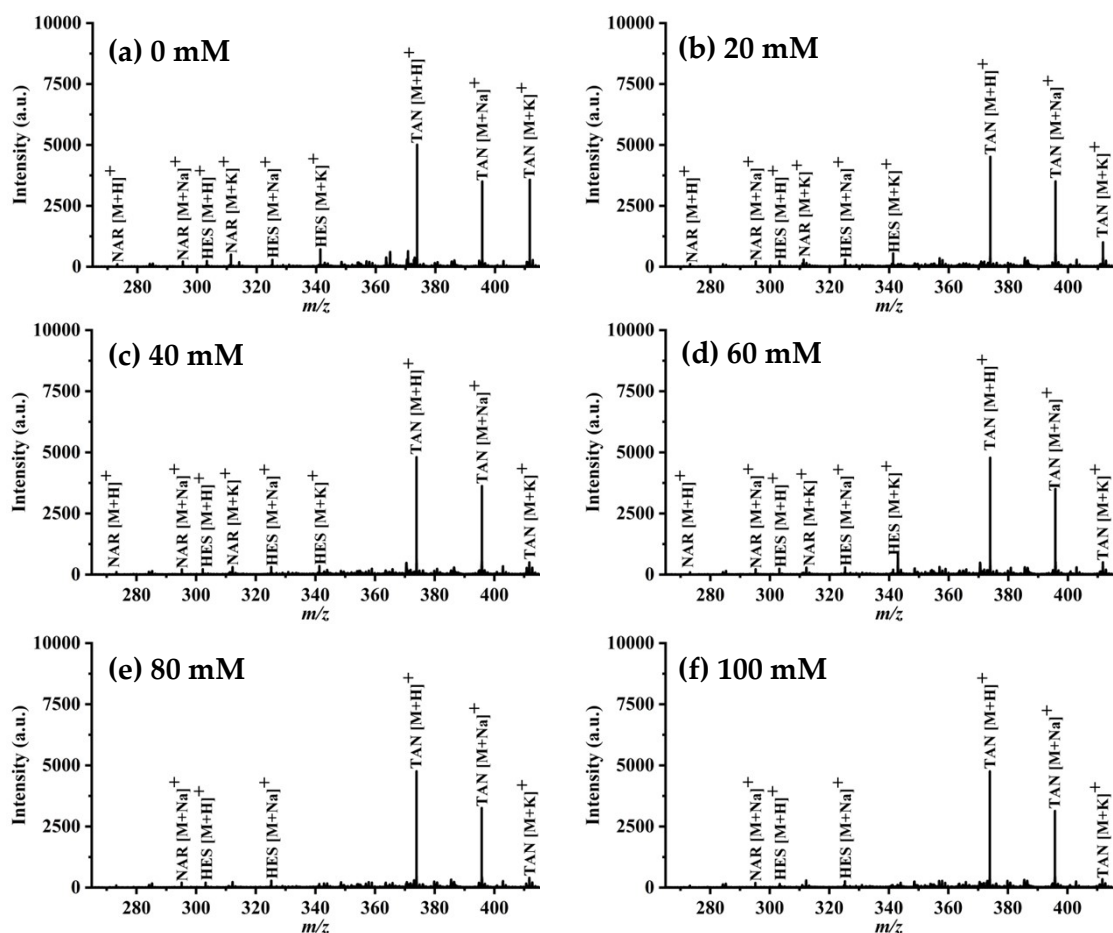
Fig. S8. MALDI-TOF-MS spectra of 100 μg/mL of tangeretin analyzed using MOF@HOF as a matrix in positive ion mode with addition of 0, 20, 40, 60, 80, and 100 mM of NaCl.
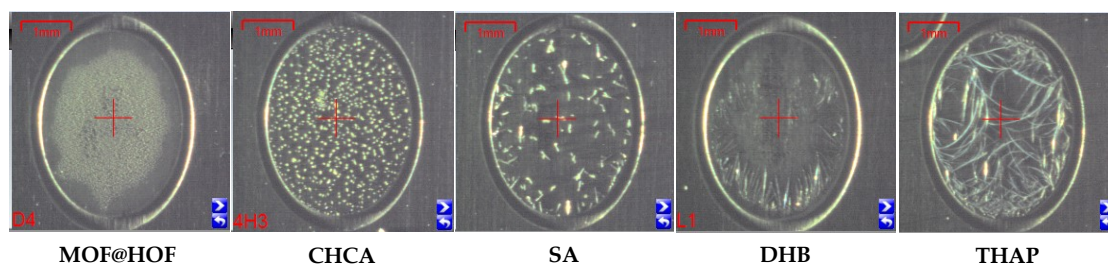
Fig. S9. Optical images of different matrix (2 mg/mL) dispersed on the stainless-steel targets. **CHCA**, α-cyano-4-hydroxycinnamic acid; **DHB**, 2, 5-dihydroxybenzoic acid; **MOF@HOF**, metal-organic framework @ hydrogen-bond framework; **SA**, sinapic acid; **THAP**, 2, 4, 6-trihydroxyacetophenone.
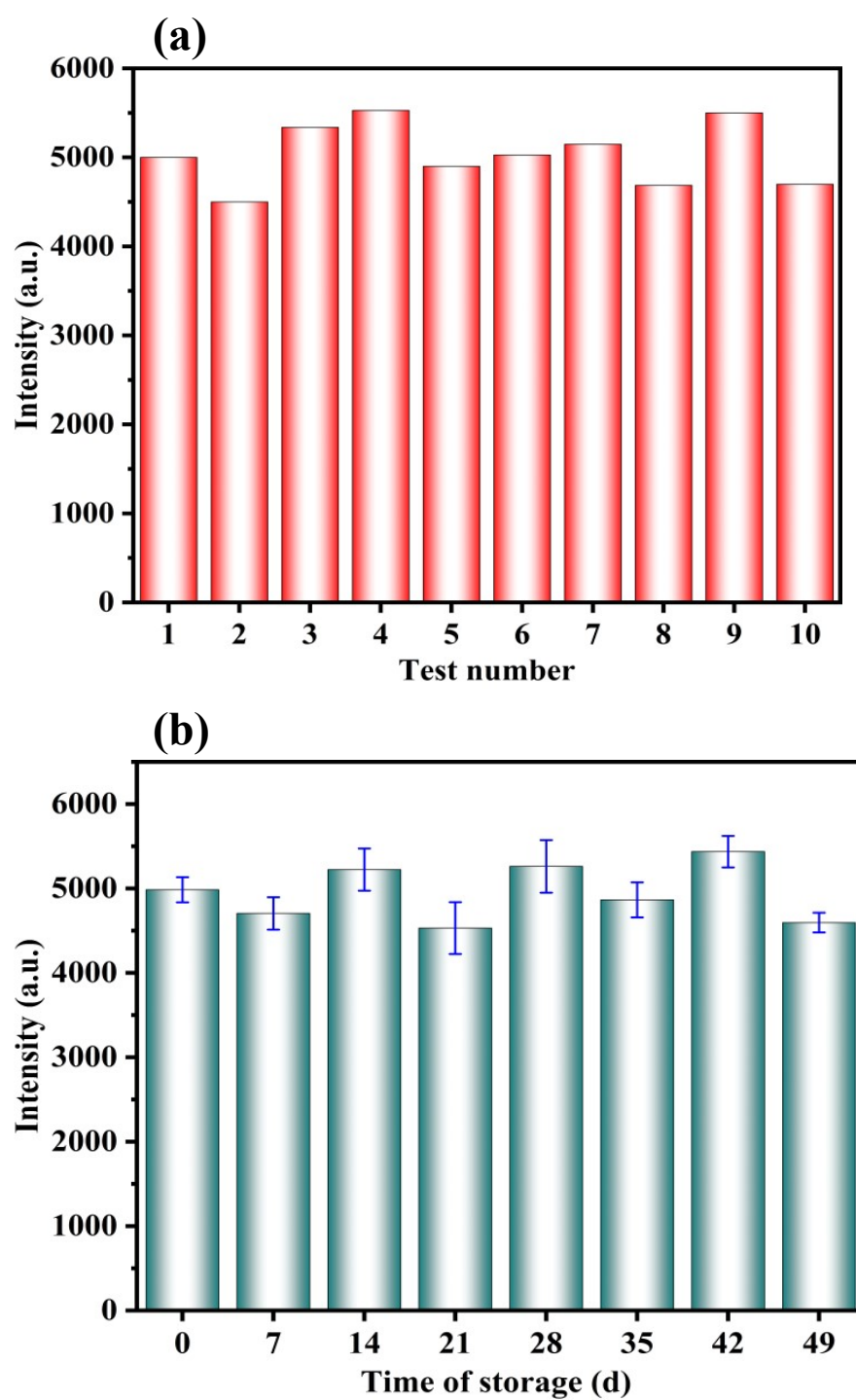
Fig. S10. (**a**) Repeatability and (**b**) storage stability test of MOF@HOF composite, based on the intensity of tangeretin ([M+H]$^+$ at m/z 373).
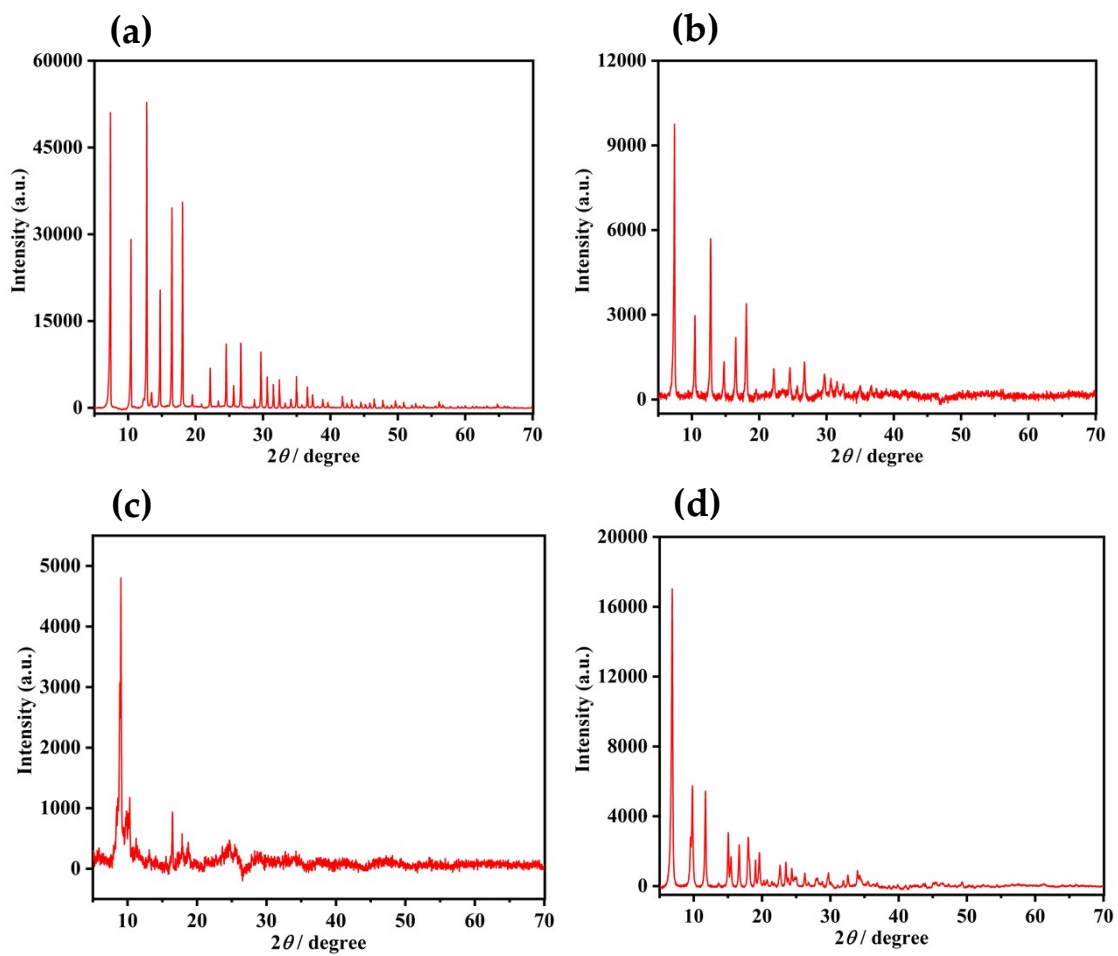
Fig. S11. The XRD spectra of (**a**) ZIF-8, (**b**) ZIF-67, (**c**) NH$_2$-MIL-101, and (**d**) NH$_2$-MIL-125.
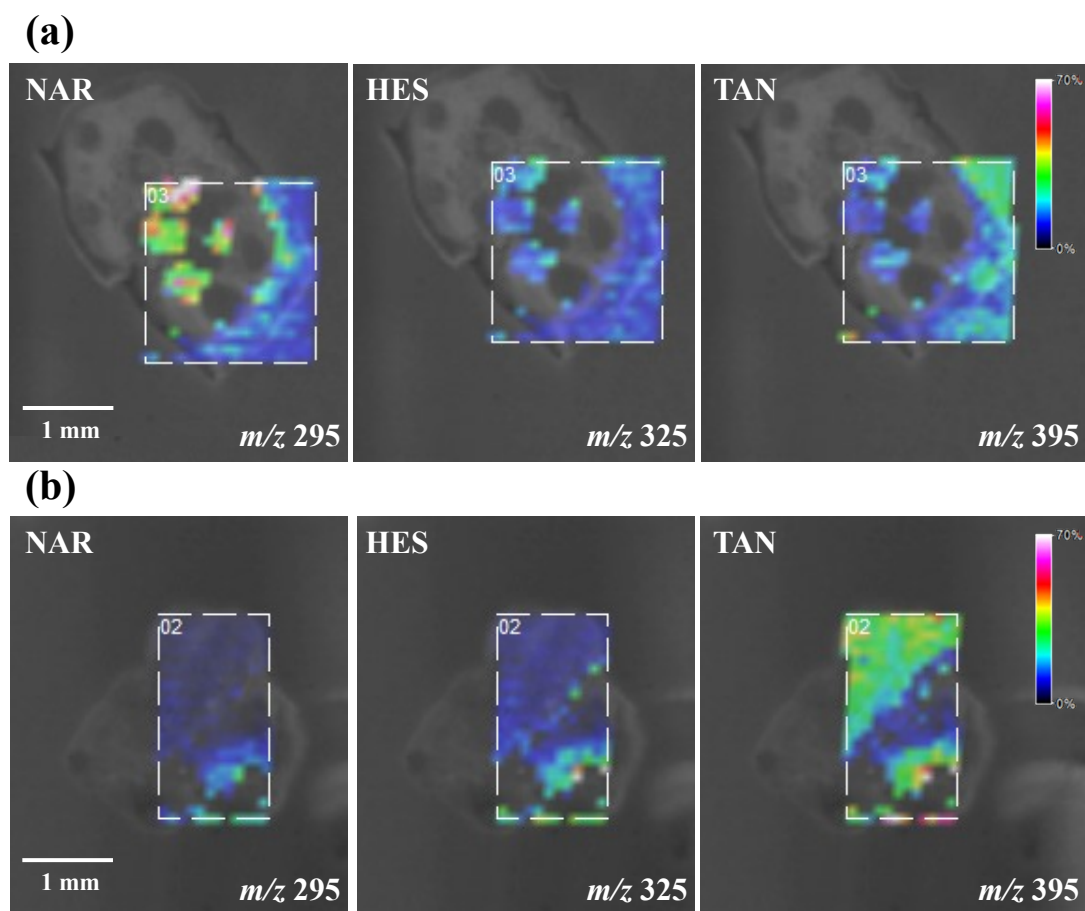
Fig. S12. MALDI-MS imaging analysis of the NAR, HES, and TAN distribution in the peel tissue of **(a)** kumquat and **(b)** honey orange. TAN, tangeretin; HES, hesperetin; NAR, naringenin.